Atmos. Chem. Phys. Discuss., 11, 4807–4842, 2011
www.atmos-chem-phys-discuss.net/11/4807/2011/
doi:10.5194/acpd-11-4807-2011

Atmospheric Chemistry and Physics Discussions

Atmospheric boundary layer characteristics over the Pearl River Delta, China during summer 2006: measurement and model results

S. J. Fan[1], Q. Fan[1], W. Yu[1], X. Y. Luo[1], B. M. Wang[1], L. L. Song[2], and K. L. Leong[3]

[1]Department of Atmospheric Sciences, Sun yat-sen University, Guangzhou, 510275, China
[2]Climate Center of Guangdong Province, Guangzhou, 510080, China
[3]Macao Meteorological and Geophysical Bureau, Macao, China

Received: 6 July 2010 – Accepted: 16 December 2010 – Published: 9 February 2011

Correspondence to: Q. Fan (eesfq@mail.sysu.edu.cn)

Published by Copernicus Publications on behalf of the European Geosciences Union.

Abstract

Atmospheric conditions are often connected with the occurrence of high pollution episodes especially in urban areas. As part of the PRIDE-PRD2006 intensive campaign, atmospheric boundary layer (ABL) measurements were carried out at Qingyuan, Panyu and Xinken in the Pearl River Delta (PRD) from 1 July to 30 July of 2006. It was found that in summer, the surface winds in PRD are more controlled by the south, and there usually is vertical wind shear at the height of 800 m or so, therefore, PRD is often influenced by the tropical cyclone/typhoon. The subsidence and precipitation from a tropical cyclone will affect the air quality of PRD. Under the subsidence, the wind speed in ABL and the height of ABL will decrease and result in high level concentrations. When the background wind speed is small or calm, the wind profile at Panyu and Xinken change dramatically with height, which is perhaps caused by the local circulations, such as the sea land breeze. For more understanding about the ABL of PRD, the simulations by the WRF mesoscale model were used to analyse the ABL characteristics in PRD. From three kinds of weather condition simulations (subsidence days, rainy days and sunny days) by WRF model, it was found that the simulated temperature, wind fields in these three cases were moderately consistent with the measurements. The results show that the diurnal variation of ABL in subsidence days and sunny days are obvious, but the diurnal variation of ABL on rainy days is not obvious. The ABL is obviously affected by the local circulation and the features of ABL are different in various stations. A simulation focus on high pollution episode during the subsidence days from 12–15 July 2006, occurred under high pressure conditions, accompanied by a tropical cyclone "Bilis". Comparing the simulated vertical wind fields and temperature structure with the ABL measurements at Xinken, Panyu and Qingyuan station, it was found that, the modelled and measured atmospheric fields reveal that there are two different kinds of ABL characteristics in PRD: when the surface winds in PRD were light or almost calm, the local circulation was dominated, such as the sea-land breeze at Xinken station and the mountain-valley circulation at Qingyuan station. When the

ACPD

11, 4807–4842, 2011

surface winds were strong, the stations were under the same background weather system and the wind directions were almost the same. Furthermore, the modelled results also suggest that the high Air Pollutant index (API) episode was caused predominately by subsidence.

1 Introduction

The Pearl River Delta (PRD), China is situated in the middle of Guangdong province, China, one of the third largest Gross Domestic Product in China. It is a coastal, industrial area situated in a region of very complex wind regimes (Chen et al., 2009; Ding et al., 2004; Liu et al., 2002). The south of Guangdong province is facing the South China Sea, in the north is the Nan Ling Mountain and in the centre is PRD, a rapidly growing area with more than 100 million people (Fig. 1a and b). PRD contains many cities, including the city of Guangzhou, Shenzhen, Foshan, Dongguan, Huizhou, Jiangmen, Zhongshan and Zhuhai, sometimes including Hongkong and Macao. There have been several investigations on the characteristics of atmospheric boundary layer (ABL) over PRD from the 1980s to 1990s (Huang and Liu, 1985; Guo, 1991; Liang et al., 1992). But in the last two decades, PRD region has experienced a period of rapid economic development and urban expansion. The land use and land cover have dramatically changed. In order to reveal the meteorological and chemical characteristics in PRD recently, "Programme of Regional Integrated Experiments of Air Quality over the Pearl River Delta" (PRIDE-PRD) campaign 2004 and 2006 were conducted and a number of researches focused on these experimental results (Hua et al., 2008; Garland et al., 2008; Li et al., 2010; Lou et al., 2010; Yu et al., 2010; Verma et al., 2009; Miyazaki et al., 2009; Zhang et al, 2008a,b; Cheng et al., 2008a). Many results pointed out that the meteorological fields were closely interacting with the chemical composition, chemical reaction process and physical optical characteristics (Liu et al., 2008; Jung et al., 2009; Xiao et al., 2009; Lu et al., 2010; Zhang et al., 2008; Rose et al., 2010; Cheng et al.,

ACPD
11, 4807–4842, 2011

2008b). The characteristics of the wind, humidity and thermodynamic conditions are essential to the air quality problem.

The ABL measurements were a very important part of these two intensive campaigns. The characteristics of ABL observations at Qingyuan, Panyu and Xinken in PRD in October 2004 were analysed in a previous study (Fan et al., 2008). The observational results showed that a surface high-pressure system (anti-cyclone), descent motion outside of Typhoon and sea breeze would result in the high-level concentrations. The presence of anti-cyclone high-pressure systems and sea breeze lead to the formation of three inversion layers and two aerosol layers as well as quite specific vertical profiles of the wind velocity over Xinken station. This study was based on the observations from 3 stations only. Limited to the resolution of the observations, it cannot present the detailed horizontal and vertical characteristics of ABL in PRD regions. Compared to the investigation of Fan et al. (2008), besides the analysis of measurements, a numerical simulation of the local circulation in PRD region was conducted. For this purpose, we applied the WRF (WRF, http://www.wrf-model.org/index.php; Skamarock et al., 2007) model that simulates atmospheric circulation at a regional scale in this paper.

The vertical structure, as well as the spatial and temporal variability of the ABL, is very important in numerical weather prediction (NWP). Many researches have demonstrated that many meteorological characteristics in the ABL can be represented by MM5 or WRF mesoscale models (Kwun et al., 2009; Zhu, 2008; Miao et al., 2009). Furthermore, accurate depiction of meteorological conditions within the ABL is also important for air pollution modelling. Knowledge of the temperature, the wind, the mixing layer height, the turbulent kinetic energy (TKE) and the horizontal or vertical circulation are all essential, especially in cases of server air pollution episodes (Prtenjak et al., 2009; Hanna et al., 2010; Gilliam et al., 2010; Hu et al., 2010). Results from some model studies (Feng et al., 2007; Wu et al., 2005) also showed that most severe air pollution episodes in PRD region are very often associated with the subsidence by tropical cyclone or sea-land breeze. Their studies (Feng et al., 2007; Wu et al., 2005)

ACPD
11, 4807–4842, 2011

also pointed out the Typhoon caused a strong descending motion in the lower troposphere, weak surface winds and a relatively low ABL. However, their study was based on simulations provided by MM5 or WRF model at a horizontal resolution of 12 km. Thus, it did not offer a detailed insight in the fine-scale lower-tropospheric conditions, which we have succeeded in doing in this study. Another novelty of this study is that we utilized WRF model results at $1\times1\,km^2$ resolution. A lot of researches pointed out that the high resolution forecast was a key task for further progress in NWP model development (Mayer et al., 2010; Jury et al., 2009; Nolan et al., 2009a,b).

In this study, we investigate the detailed characteristics of ABL in summer 2006 in PRD region. We especially focus on three kinds of weather, one is the tropical cyclone process which occurred on 12–15 July 2006, resulting in a high air pollution index (API) pollution episode. The second period is the rainy days from 14–18 July and the third is the sunny days from 20–23 July. WRF model was utilized to investigate the features of ABL in these three periods. The simulation results are compared with the observations. Besides various horizontal and vertical meteorological fields, the local circulations are also analysed. In Sect. 2, the field experimental set up and synoptic situations are described. The model settings and model results obtained from the three-dimensional numerical simulations are involved in Sect. 3. Conclusions will follow in the last Sect. 4.

2 Experimental set up and synoptic situations

2.1 Experimental set up

The selected PRD intensive campaign period was in summer. In this period of the year, lower pressure synoptic systems dominate and the PRD region usually experiences pollution episodes by the Typhoon's strong descending motion (Feng et al., 2007; Wu et al., 2005). The campaign began on 1 July 2006 and ended on 30 July 2006. In order to study the characteristics of ABL over PRD area, five observational sites were selected, as shown in Fig. 1b, Qingyuan, Guangzhou back garden, Guangzhou,

ACPD
11, 4807–4842, 2011

Panyu and Xinken. In these stations, Qingyuan, Panyu and Xinken conducted the sounding observation. Panyu station was located at Panyu meteorological Bureau (22.56° N, 113.19° E), about 20 km south from Central Guangzhou, in the middle of PRD. Qingyuan station was located in Qingyuan meteorological bureau (23.40° N, 113.03° E), in the north of PRD. Xinken station was located in Xinken town (22.37° N, 113.35° E), in the south of PRD. Qingyuan and Xinken represent a more rural environment. At Qingyuan station, vertical measurements were made with meteorological radar. Mean wind speed and direction, temperature and relative humidity were automatically derived from radio soundings. These parametres were reported several times per day between 0 and 3000 m with a vertical resolution of 100 m. At Panyu and Xinken stations, radio soundings were performed to obtain mean velocity, wind direction and temperature. Radio soundings were launched seven times (06:00, 08:00, 10:00, 14:00, 18:00, 20:00, 23:00 LST) or eleven times (intensive observation, 02:00, 06:00, 07:00, 08:00, 10:00, 14:00, 17:00, 18:00, 19:00, 20:00, 23:00 LST) per day. Mean wind speed and direction were given between 0 and 2000 m with a vertical resolution of 50 m, while mean temperature was reported with a vertical resolution of 10 m.

Guangzhou back garden and Guangzhou station conducted an automatic weather station by obtaining hourly wind speed, wind direction, temperature, radiation and relative humidity. Guangzhou back garden station was located in Guangzhou back garden (23.55° N, 113.07° E), about 50 km north from the Central Guangzhou. Guangzhou station was located on the 16th floor (50 m a.g.l.) of the Guangdong Provincial Environmental Monitoring Center (GPEMC) building (23.13° N, 113.26° E).

2.2 Weather conditions in July 2006

According to the Central Meteorological Station of Guangdong province, meteorological conditions over PRD in July 2006 were characterised by high temperature and much precipitation. Figure 2 shows the measured temperature, precipitation and API at Guangzhou station during July 2006. There were two periods of high temperature weather from 12–14 July and 23–25 July, corresponding to strong tropical cyclone

ACPD
11, 4807–4842, 2011

"Bilis" and typhoon "Kaemi", respectively. There were also two peaks in API values influenced by these two tropical cyclone processes. Two strong precipitation processes occurred in 15–17 July and 26–30 July. In other sunny days, the whole PRD regions were more dominated by the subtropical high pressure. It was found that in July 2006, the surface winds in PRD are more controlled by the south, and the winds sometimes veer to north from midnight to morning in the north areas in PRD. There was usually vertical wind shear at the height of 800 m or so. The influence of sea-land breeze is obvious in the south of PRD, besides, this region is often affected by the Tropical cyclone in summer. The subsidence and precipitation from a tropical cyclone are vital to the air quality in PRD. The wind speed in the ABL and the ABL height will decrease under subsidence, which will result in the air pollution episode. The analysis from the sounding data in this experiment show that when the background wind speed is small or calm, the wind fields at Panyu and Xinken station change dramatically with height, which is perhaps caused by the local circulations, such as the heat island circulation and the sea-land breeze. The wind profile at Panyu station is very complex with the subsidence. So in this study, we will discuss these three kinds of ABL features in PRD. As shown in Fig. 2, period I belongs to the subsidence days from 12–15 July, period II corresponds to the rainy days from 15–18 July and period III is the sunny days from 20–22 July. As stated in the introduction, many researches (Feng et al., 2007; Wu et al., 2005) have already pointed out that the strong descending motion can result in the high pollution weather in PRD. The two API peaks in this July were also caused by the subsidence motion from tropical cyclones. So we will especially focus on the ABL characteristics in PRD from 12–15 July, the detail synoptic situation during this period were illustrated in the following.

Influenced by subtropical high pressure and subsidence by strong tropical cyclone "Bilis", it appeared as high temperature in PRD region from 12–14 July, the maximum temperature exceeded 32 °C in these three days. Figure 3 shows the surface weather situation during 12–15 July. Bilis originally formed from a tropical depression on 9 July 2006 over the Western North Pacific. It intensified from a tropical storm to a severe

ACPD
11, 4807–4842, 2011

tropical storm at 14:00 LST on 11 July. It made landfall at Yilan in Taiwan at midnight on 13 July and then tracked northwest. It then landed at Xiapu in Fujian province at 12:00 LST on 14 July. PRD region was west or southwest of Bilis during its movement.

3 Model results

3.1 WRF model and settings

To study the event, WRF mesoscale model was employed. The WRF model consists of fully compressible nonhydrostatic equations on a staggered Arakawa C grid. Its vertical coordinate is a terrain-following hydrostatic pressure coordinate. The Runge-Kutta 3rd order time integration scheme and 5th order advection schemes in a horizontal direction and the 3rd order in vertical ones are used. A time-split small step for acoustic and gravity-wave modes is utilized. In this study, four domains (Fig. 4), all centred at Pearl River Estuary, are configured with a horizontal grid of 139×91, 181×148, 322×223 and 367×277 points and a resolution of 27, 9, 3, 1 km, respectively. The central latitude and longitude of the coarse domain (D01) were 23° N and 113° E. Two-way nesting were applied for the domains. For the model to adequately resolve the boundary layer processes, from the top to the surface level, there were 35 sigma levels in the vertical. Twenty layers were below a height of 2 km. The most fine topography input was extracted from the 30″-resolution global terrain and land use files. The original USGS 24-category land cover data was employed.

The main physics options included Lin et al. microphysics; the Betts-Miller-Janjic cumulus parameterization; the RRTM longwave radiation scheme; the Goddard shortwave radiation scheme and MRF boundary layer scheme. For the two inner domains (D03 and D04), it was assumed that the convection was reasonably well resolved by the explicit microphysical parameterization scheme and no cumulus parameterization scheme was used.

ACPD
11, 4807–4842, 2011

In order to represent the different ABL features, three kinds of weather were chosen. The first simulation period (period I) was from 00:00 UTC 12 July 2006 to 00:00 UTC 15 July 2006, corresponding to the subsidence days. The second simulation (period II) began at 00:00 UTC 14 July 2006 and ended at 00:00 UTC 18 July 2006, this period represented the rainy days. The third simulation period was from 00:00 UTC 20 July 2006 to 00:00 UTC 23 July 2006, corresponding to the sunny days. In all these simulations, the lateral and initial conditions for WRF simulations were obtained from NCEP/NCAR reanalysis daily $1^{\circ}\times1^{\circ}$ grid data. In this study, 12 h were used for the spinning up time.

3.2 Model results

For more understanding about the summer boundary layer characteristics of PRD, A WRF mesoscale model was employed to study the detail horizontal and vertical characteristics of ABL in PRD.

3.2.1 Measured vs. modelled data

In order to validate the WRF simulation results, the model results were compared with the available surface observations furnished by the main meteorological stations in domain 4 (shown in Fig. 4). Table 1 show some commonly statistical variables used to evaluate the performance of model simulations, including the correlation coefficients (R), mean bias (MB), mean absolute gross error (MAGE), root mean squared error (RMSE), and fractional absolute error (FAE). MB, MAGE, RMSE, and FAE are defined as follows (Yu et al., 2005):

$$\mathrm{MB} = \frac{1}{MN}\sum_{j=1}^{M}\sum_{k=1}^{N}\left(C_{j,k}^{\mathrm{m}} - C_{j,k}^{\mathrm{o}}\right) \quad \mathrm{MAGE} = \frac{1}{MN}\sum_{j=1}^{M}\sum_{k=1}^{N}\left|C_{j,k}^{\mathrm{m}} - C_{j,k}^{\mathrm{o}}\right|$$

ACPD
11, 4807–4842, 2011

$$\mathrm{RMSE} = \frac{1}{M}\sum_{j=1}^{M}\left[\frac{1}{N}\sum_{k=1}^{N}(C_{j,k}^{\mathrm{m}} - C_{j,k}^{\mathrm{o}})^2\right]^{1/2} \qquad \mathrm{FAE} = \frac{1}{MN}\sum_{j=1}^{M}\sum_{k=1}^{N}\frac{\left|C_{j,k}^{\mathrm{m}} - C_{j,k}^{\mathrm{o}}\right|}{(C_{j,k}^{\mathrm{m}} + C_{j,k}^{\mathrm{o}})/2}$$

Where M is the number of stations and N is the number of numerical hours excluding the spinning up time, C^{m} and C^{o} represent the modelled and the observed values, respectively. From the definitions above, the MB, MAGE, RMSE, and FAE are more near zero, the model simulations best. It should be noted in Table 1 that except for the wind speed in period II, the average simulated wind direction, wind speed and temperature in three periods are all close to the observations. There are good correlations between the simulated temperature and the observations in period I and period III, with the correlation coefficient reaching 0.72 and 0.91, respectively. The values of MB, MAGE, RMSE, and FAE with respect to temperature are −1.08, 1.80, and 2.19 °C and 1.5% in period I and −1.26, 1.31, and 1.63 °C and 1.2% in period III, indicating a good overall agreement between the observations and the simulations. For wind speed and wind directions in three periods, the correlation coefficients are all about 0.4 and the values of MB, MAGE, RMSE, and FAE indicated the model overestimated the wind fields in most of the time. It should be mentioned that because of the vector characteristics of wind directions, MB, MAGE, RMSE, and FAE for wind directions were calculated by finding the actual differences in the angle between modelled directions and observed directions. In all, the simulated results in the subsidence days (period I) and in sunny days (period III) are better than those in the rainy days (period II).

The time series of the hourly 2-m temperature, 10-m wind speed and wind direction observed at Guangzhou station from 12 to 15 July (period I), and the corresponding simulations, are shown in Fig. 5. It can be seen that the model performed generally well in the simulations of the diurnal variation tendency of air surface temperature. The increase of temperature during 14 July was captured well by WRF model, but the model tended to under predict the temperature especially from 12 July to 13 July and in 15 July. In the case of wind speed, WRF simulations were in moderate agreement with the observations in terms of diurnal variations and magnitudes during most time.

ACPD
11, 4807–4842, 2011

Compared with the measurements, the simulated wind speeds were a little lower during 13 July and slightly higher after the night of 14 July. Regarding the wind directions, the observed and simulated winds were all from the west during the simulation period. WRF model achieved good results except at noon of 13 July. At that time, the observed wind direction was northwest, but the simulated result was from the east. Except for that time, the wind direction results were satisfied.

3.2.2 Atmospheric boundary layer heights

The ABL height is a critical parameter for vertical dispersion. Accurate assessment of boundary layer information on a finer scale should improve the ability to assess the pollutant diffusion process. The variation of the modelled WRF ABL height for Qingyuan, Back garden, Guangzhou, Panyu and Xinken stations (Fig. 1b) during three simulation periods and the lidar normalized relative backscattering signal observed at YuenLong station in Hongkong are shown in Fig. 6.

In all the five stations, the simulated diurnal variation of ABL height in subsidence days and sunny days were all more obvious than those in rainy days. In rainy days, the change of ABL height was instantaneous, the ABL changed quickly from the stable regime to the convection regime. But in subsidence days and sunny days, the ABL were of a nocturnal regime in the nighttime and a free convection regime when there has strong heating from below. It also can be seen from the lidar normalized relative backscattering signal observed at YuenLong station in Hongkong. These lidar measurements are from Hongkong University of science and technology. The observations by lidar also showed that there were obvious diurnal changes of ABL height in subsidence days and sunny days. In the rainy days, the diurnal variation was not apparent.

The daily evolutions and magnitude of ABL height at Xinken station were all different from the other four stations. The ABL heights in three simulation periods at Xinken station were much lower than those in the other stations and the diurnal variations of ABL height at Xinken stations were also not clear. In the other four stations, it can be seen that the development of a well-mixed layer begins 08:00–09:00 LST, e.g.,

ACPD
11, 4807–4842, 2011

2–3 h after the sunrise, reaching up to the maximum (1500 m) at about 14:00 LST. Whereas in the nighttime, the ABL are most stable, with the heights all lower than several hundred metres. Compared with these four stations, the daily evolutions of the ABL height at Xinken are very special. For example, in the subsidence days, the daily maximum of ABL height at Xinken was around 400 m at 08:00 LST, which was much lower than those in other stations. The occurrence time was also earlier. Besides, the ABL height at Xinken from 09:00 LST on 13 July to 07:00 LST on 14 July maintained a very low value. The ABL was of static stability, which was beneficial to the high pollution episode. From the wind profile measurements, the vertical wind direction and wind speed changed dramatically in these two days at Xinken. It could have caused the ABL height at Xinken to have been lower than those in other stations. The wind fields at Xinken were complex because it locates in the Pearl River Estuary. Besides the system wind, it is also affected by the local circulation, such as sea-land breeze.

The simulated ABL heights during the night of subsidence days were much lower than those in other days. Influenced by the descent motion, the ABL is stable and the ABL height will be decreased. The observations from lidar signals showed that the maximum ABL height in the daytime reached 1500 m or so, and the ABL height during the night of subsidence days dropped to several hundred metres. WRF model can capture the diurnal variation tendency of ABL height and the simulated ABL heights in the daytime were moderately consistent with the lidar results, but the heights in nighttime were much lower than the measurements. In some stations, the simulated ABL heights were near zero. It was caused by the MRF high resolution planetary boundary layer parameterization scheme used in the model. The ABL heights calculated by this scheme in the nighttime were much lower.

Figure 7 shows measured air pollutant concentrations at Guangzhou station from 13 July to 22 July. Comparing the simulated ABL height results with the observed air concentrations, it can be seen that the temporal variations of air concentrations were related to the meteorological conditions closely. From 13 July to 14 July, when the ABL height was high, the air concentrations were comparatively low under the good diffusion

ACPD
11, 4807–4842, 2011

condition, and vice verse. During this episode, PRD area was under the influence of a subtropical high pressure system and a tropical cyclone "Bilis". The combination of the low ABL height, the strong descent motion and the weak surface wind acts to keep the pollutants in the ABL and leading to comparatively high API values. During period II from 15 July to 17 July, the air concentrations had all decreased due to the wet deposition by precipitation process. In the sunny days from 21 July to 22 July, the air concentrations appeared as obvious diurnal variations again. When the ABL is stable and the ABL height is low, this results in high air concentrations.

3.2.3 Vertical wind and temperature distribution features

The vertical radio sounding measure experiments were conducted at Panyu and Xinken stations during July in 2006. Besides, the vertical measurements were made with meteorological radar at Qingyuan station in order to explore the ABL features in different regions. Due to various reasons, the sounding data at these three stations in this month were inadequate. According to the actual corrected data in our three simulation periods, the vertical wind profile at Panyu station and the vertical temperature profile at Qingyuan station on 14 July and 21 July were analysed in the following.

The vertical wind profile measured at Panyu station and the simulated results by WRF model on 14 July and 21 July are shown in Fig. 8. The sounding measures were cancelled on the rainy day, so the measurements on the subsidence day and sunny day were used to compare. It can be seen that there have been obvious discrepancies in the vertical wind fields during the subsidence day and the sunny day. The wind under the ABL at Panyu station was from the west all day on 14 July and there had been the low jet at about 500 m height at 06:00 LST. The wind is from the southwest near the surface and veered to the west at a very low height. The ABL height at that time was very low. The modelled ABL height in the WRF model was also very low in Fig. 6. At 16:00 LST and 17:00 LST, the wind in all the ABLs changed to southwest. The model results in Fig. 8b can capture the ABL characteristics quite well except for the near surface. The temporal resolution of WRF model is higher than that in the measurements,

ACPD
11, 4807–4842, 2011

the ABL features can be illustrated by model results more clearly. The wind speed increased from 00:00 LST in 14 July and reached the maximum at about 07:00 LST. The maxima speed located at several hundred metres high. The wind direction was almost northwest which corresponded with the measurements. After 10:00 LST, the wind speed began to decrease and maintained for about 7 h. At 17:00 LST, the wind speed increased again and veered to the southwest. In Fig. 8c, the wind profile was complex. On the morning of 21 July, the wind directions changed dramatically with height. Wind directions above 1000 m were mainly southeasterly and below 1000 m southwest. At 14:00 LST, the wind in all the ABLs was almost from the south. After 16:00 LST, the wind veered to the southeast. The model results in Fig. 8d can reproduce the features explored by the measurements. At the beginning of 21 July, the wind in the low ABL was southwesterly and the wind changed to southeast after 16:00 LST. At 06:00 LST, the southwest wind veered to the south with the height. The minimum wind speed occurred at noon of 21 July. The wind speed increased after 16:00 LST and the wind direction higher than 1000 m had changed to the east at 23:00 LST. In general, the wind profiles reproduced by WRF model were satisfied. In subsidence day and sunny day, the wind profiles at Panyu station were all very complex. The wind speed and direction changed very fast, which was mainly caused by the local circulation.

Figure 9 shows the measured vertical temperature distribution by radar sounding and the modelled results at Qingyuan station on 14 July and 21 July. On 14 July, WRF model can capture the decreasing of temperature with the height at three times, especially below 1000 m. From 1000 m to 3000 m, the model overestimated the temperature about 1–2 °C. At 07:00 LST on 21 July, the model results were consistent with the measurements. At 17:00 LST and 19:00 LST on 21 July, the model also reproduced the measurement well below 1000 m, but above 1000 m the model underestimated the measurements. During these two periods, there was a little inversion at 1500 m at Qingyuan station. It can also be seen in the model results that the temperature increased with the height at about 1500 m, but the actual temperature values were lower than the measurements.

ACPD
11, 4807–4842, 2011

3.2.4 Horizontal wind fields from 12 July to 14 July

As stated in Sect. 3.2.1, the temperature, wind fields simulated by the WRF model were moderately consistent with the measurements during the subsidence days, rainy days and sunny days. Among these three kinds of weather, the subsidence days were the most important to the diffusion of air pollutants. The detailed simulated horizontal wind fields and the vertical circulation by WRF model during the subsidence days were analysed in the following.

Figure 10a and b show the observed and simulated 10-m wind vectors in PRD region at 20:00 LST on 12 July and at 02:00 LST on 13 July. They clearly show that different local circulations dominated PRD regions, and the wind vectors were various at different stations. It can be seen from Fig. 10a that at Xinken station, located in the Pearl River Estuary, the winds were from the south. It was obviously influenced by the sea breeze. At Panyu station, about 20 km south from Central Guangzhou, the wind direction was southeast and the wind speed decreased. At Guangzhou station, in the urban centre, the wind veered toward the east and the wind speed increased. At Guangzhou back garden station, the wind speed decreased again. At Qingyuan station, the wind changed to south. The simulated wind fields were almost consistent with the observations. The wind speeds at Xinken and Guangzhou stations were larger than other stations. At 00:00 LST on 13 July (Fig. 10b), the wind speeds were smaller than those at 20:00 LST on 12 July (Fig. 10a), the local circulations were also very obvious. The winds at Xinken station changed to the west, it was also affected by the sea-land breeze. At Panyu and Guangzhou stations, the wind directions were still from the west, but the wind speeds decreased. At Guangzhou back garden station, the winds veered to the east and at Qingyuan station the winds changed to southeast. These two stations were influenced by the local circulation, different from the other three stations. At that time, the tropical cyclone "Bilis" still had not made landfall, the distance between "Bilis" and PRD region was far. The average wind speed at Guangzhou on 12 July was 1.54 m s^{-1}. Under the small background system wind fields, the local circulation

ACPD
11, 4807–4842, 2011

is essential to various stations. Figure 10c and d shows the observed and simulated wind vectors in PRD region at 08:00 LST on 14 July and 14:00 LST on 14 July. Different from Fig. 10a and b, the wind fields at various stations seem very similar. In Fig. 10c, the aforementioned stations were all controlled by west. At that time, the tropical cyclone "Bilis" had already made landfall, PRD regions were deeply influenced by "Bilis". The average wind speed at Guangzhou in 14 July was 3.46 m s^{-1}. The winds at various stations in PRD tend to be similar under such background system wind fields. The winds in Fig. 10d were almost northwest. The wind direction in Qingyuan station was southwest, because it locates in the south of Nanling Mountain areas, which was influenced by the downstream flow from the slopes of the high mountains.

3.2.5 Vertical circulation from 12 July to 14 July

Modelled vertical cross-sections of wind vectors along 113.2° E at 03:00 LST on 13 July and 03:00 LST on 14 July are presented in Fig. 11. Here, the analysis is concentrated on the local circulation. At 03:00 LST on 13 July (Fig. 11a) different wind fields can be noted near the coast compared to adjacent urban cities. As mentioned above, when the system wind speed is small, the local circulation is essential to various stations. In this episode, the tropical cyclone "Bilis" made landfall at midnight on 13 July. The influence from "Bilis" was not very apparent in PRD region at 03:00 LST on 13 July. Figure 11a shows the coastal areas (such as Pearl River Estuary, about 22.2° N) were dominated by the south. The surface layer was under the influence of the incoming sea breeze. The air converged and ascended in the coastal region. The wind direction veered toward the north at 900 hPa. There was an obvious sea-land breeze circulation. The wind fields were influenced by the urban heat island circulation at Panyu and Guangzhou station. The heat island circulation was comparatively complex. The ascend motion and descend motion were weak, the horizontal south (near surface) and north wind fields (850 hPa or so) were apparent. Compared with the coastal areas, the urban regions were under the control of divergence, and resulted in stable and low ABL layer. The wind direction in Qingyuan station (about 23.4° N) was also south, but

ACPD
11, 4807–4842, 2011

with the ascend motion in the high vertical latitude. It seems that there was another circulation affecting the wind fields in Qianyuan. The north of Qianyuan is Nanling Mountain (about 25° N), the flow from the south encounters the mountains and uplifts, then veers to the north at high latitude and descends. Qingyuan is always affected by the mountain-valley wind from the slopes of the high mountains. Overall, when the system wind is weak, there were three kinds of local circulations: sea-land breeze, urban heat island and mountain valley in PRD regions. These local circulations make the characteristics of ABL in PRD unique.

When the system wind is moderate, the wind fields in PRD regions tend to be similar. At 03:00 LST on 14 July (Fig. 11b), the tropical cyclone "Bilis" has already made landfall and decreased, PRD region was located in the southwest of the cyclone. The whole PRD region was controlled by the north wind in the low troposphere. The discrepancy between different stations was almost ignored.

4 Conclusions

The characteristics of ABL at different sites in PRD were analysed by measurements and model results from mesoscale model WRF during three kinds of weather, especially focusing on a comparatively high API episode during 12–15 July 2006. The results show that the characteristics of ABL at different stations are various. These local scale meteorological conditions could not be captured by 50 km and 10 km resolution meteorological model. Fine-scale (at a resolution of 1 km) meteorological (WRF) results demonstrated a successful simulation in ABL and reasonable agreement with the available observations. The main meteorological results provided by this study can be used for other studies in PRD July intensive campaign. The meteorological model results can be further used to the air quality model to perform the air concentration simulation. The temporal variation tendency of various air pollutant concentrations can also be interpreted by the detailed ABL features. The main conclusions by this study are summarized as follows.

ACPD
11, 4807–4842, 2011

– The features of ABL under three kinds of weather: subsidence days, rainy days and sunny days in July, 2006 were analysed with observations and simulations by the WRF model. The results show that the model can reproduce the meteorological fields well. The evolution of ABL in rainy days is different from those in subsidence days and sunny days. The diurnal variation of ABL height in rainy days was not apparent.

– The evolution of the ABL height at Guangzhou, Panyu, back garden and Qingyuan stations are similar. The diurnal variation process is obvious. In daytime, the ABL is convective and the maximum ABL height can reach 1500 m or so. In nighttime, the ABL turns to stable and the ABL height decrease very much, just several hundred metres. At Xinken station, the ABL height is comparatively lower than those in other stations, the wind direction and wind speed also changed dramatically from the observations.

– Compared with other days in July 2006, the temperature and API values were higher during 12–15 July. The stable and low ABL layer, the descend motion and the weak horizontal wind are also not benefit to the diffusion of air pollutants and result in the high air concentrations.

– The detailed analyses of wind regimes and thermo-dynamical structure of the lower troposphere in PRD show that there has obvious discrepancy between different sites under small background wind circumstance. The differences are induced by the local effects in PRD areas, such as sea-land breeze effects, urban heat island effects and mountain valley effects. When the system background wind speed is moderate, the differences between various sites are not apparent. The wind fields tend to be similar.

– The ABL characteristics are important to identify the air pollution problem. The ABL features are very complex in PRD region, especially in weak winds and calms, which are always accompanied by high pollutant concentrations. However,

ACPD
11, 4807–4842, 2011

the episode in this paper was characterised by extremely complex ABL, accompanied with subsidence by tropical cyclone "Bilis". Thus, simultaneous local circulations were responsible for different wind fields at various sites. Finally, it can be summarized that the local meteorological conditions were favourable for the formation of the stable ABL and the air pollution episode.

Acknowledgements. This study was supported by funds from China National Basic Research and Development Programs 2002CB410801 and 2002CB211605, National Natural Science Foundation 40805043, 40875007 and 90715031. The authors would like to acknowledge the science team of PRD July intensive campaign for their successful collaboration. And thanks the Guangdong Meteorological Bureau, in particular Y. R. Feng for providing the meteorological observations. Implemented suggestions from various anonymous reviewers contributed significantly as well.

References

Chen, X. L., Feng, Y. R., Li, J. N., Lin, W. S., Fan, S. J., Wang, A. Y., Fong, S. K., and Lin, H.: Numerical simulation on the effect of sea-land breezes on atmospheric haze over the Pearl River Delta region, Environ. Model. Assess., 14, 351–363, 2009.

Cheng, Y. F., Wiedensohler, A., Eichler, H., Su, H., Gnauk, T., Brüggemann, E., Herrmann, H., Heintzenberg, J., Slanina, J., Tuch, T., Hu, M., and Zhang, Y. H.: Aerosol optical properties and related chemical apportionment at Xinken in Pearl River Delta of China, Atmos. Environ., 42, 6351–6372, 2008a.

Cheng, Y. F., Wiedensohler, A., Eichler, H., Heintzenberg, J., Tesche, M., Ansmann, A., Wendisch, M., Su, H., Althausen, D., Herrmann, H., Gnauk, T., Brüggemann, E., Hu, M., and Zhang, Y. H.: Relative humidity dependence of aerosol optical properties and direct radiative forcing in the surface boundary layer at Xinken in Pearl River Delta of China: an observation based numerical study, Atmos. Environ., 42, 6373–6397, 2008b.

Ding, A. J., Wang, T., Zhao, M., Wang, T. J., and Li, Z. K.: Simulation of sea-land breeze and a discussion of their implication on the transport of air pollution during a multi-day ozone episode in the Pearl River Delta of China, Atmos. Environ., 38, 6737–6750, 2004.

Fan, S. J., Wang, B. M., Tesche, M., Engelmann, R., Althausen, A., Liu, J., Zhu, W., Fan, Q.,

ACPD

11, 4807–4842, 2011

Li, M. H., Ta, N., Song, L. L., and Leong, K. C.: Meteorological conditions and structures of atmospheric boundary layer in October 2004 over Pearl River Delta area, Atmos. Environ., 42, 6174–6186, 2008.

Feng, Y. R., Wang, A. Y., Wu, D. and Xu, X. D.: The influence of tropical cyclone Melor on PM_{10} concentrations during an aerosol episode over the Pearl River Delta region of China: Numerical modelling versus observational analysis, Atmos. Environ., 41, 4349–4365, 2007.

Garland, R. M., Yang, H., Schmid, O., Rose, D., Nowak, A., Achtert, P., Wiedensohler, A., Takegawa, N., Kita, K., Miyazaki, Y., Kondo, Y., Hu, M., Shao, M., Zeng, L. M., Zhang, Y. H., Andreae, M. O., and Pöschl, U.: Aerosol optical properties in a rural environment near the mega-city Guangzhou, China: implications for regional air pollution, radiative forcing and remote sensing, Atmos. Chem. Phys., 8, 5161–5186, doi:10.5194/acp-8-5161-2008, 2008.

Gilliam, C. R. and Pleim, E. J.: Performance Assessment of New Land Surface and Planetary Boundary Layer Physics in the WRF-ARW, J. Appl. Meteorol. Clim., 49, 760–774, 2010.

Guo, D. Z.: A study of the characteristics in the coastal boundary layer in the low latitude, Research of Environmental Sciences, 5, 34–39, 1991, in Chinese.

Hanna, R. S., Reen, B., Hendrick, E., Santos, L., Stauffer, D., Deng, A. J., and McQueen, J.: Comparison of observed, MM5 and WRF-NMM model-simulated, and HPAC-assumed boundary-layer meteorological variables for 3 days during the IHOP field experiment, Bound.-Lay. Meteorol., 134, 285–306, 2010.

Hu, X. M., Nielsen-Gammon, W. J., and Zhang, F. Q.: Evaluation of three planetary boundary layer schemes in the WRF model, J. Appl. Meteorol. Clim., e-View, 2010.

Hua, W., Chen, Z. M., Jie, C. Y., Kondo, Y., Hofzumahaus, A., Takegawa, N., Chang, C. C., Lu, K. D., Miyazaki, Y., Kita, K., Wang, H. L., Zhang, Y. H., and Hu, M.: Atmospheric hydrogen peroxide and organic hydroperoxides during PRIDE-PRD'06, China: their concentration, formation mechanism and contribution to secondary aerosols, Atmos. Chem. Phys., 8, 6755–6773, doi:10.5194/acp-8-6755-2008, 2008.

Huang, Z. X. and Liu, J. L.: A preliminary results of observation on sea-land breezes in Lingding Yang area, Journal of Tropical Oceanography, 3, 21–29, 1985 (in Chinese).

Kwun, J. H., Kim, Y. K., Seo, J. W., Jeong, J. H., and Sung, H. Y.: Sensitivity of MM5 and WRF mesoscale model predictions of surface winds in a typhoon to planetary boundary layer parameterizations, Nat. Hazards, 51, 63–77, 2009.

Jung, J. S., Lee, H. L., Kim, Y. J., Liu, X. G., Zhang, Y. H., Gu, J. W., and Fan, S. J.: Aerosol chemistry and the effect of aerosol water content on visibility impairment and radiative forcing

ACPD
11, 4807–4842, 2011

in Guangzhou during the 2006 Pearl River Delta campaign, J. Environ. Manage., 90, 3231–3244, 2009.

Jury, R. M., Chiao, S., and Harmsen, E. W.: Mesoscale Structure of Trade Wind Convection over Puerto Rico: Composite Observations and Numerical Simulation, Bound.-Lay. Meteorol., 132, 289–313, 2009.

Li, X., Brauers, T., Shao, M., Garland, R. M., Wagner, T., Deutschmann, T., and Wahner, A.: MAX-DOAS measurements in southern China: retrieval of aerosol extinctions and validation using ground-based in-situ data, Atmos. Chem. Phys., 10, 2079–2089, doi:10.5194/acp-10-2079-2010, 2010.

Liang, H. M., Dong, B. Q., and Tian, G. S.: The characteristics analysis of the stratification in the ambient air over Pearl River Delta area, Research of Environmental Sciences, 4, 8–14, 1992, in Chinese.

Liu, H. P. and Chan, J. C. L.: An investigation of air-pollution patterns under sea-land breezes during a server air-pollution episode in Hong Kong, Atmos. Environ., 36, 591–601, 2002.

Liu, X. G., Cheng, Y. F., Zhang, Y. H., Jung, J. S., Sugimoto, N., Chang, S. Y., Kim, Y. J., Fan, S. J., and Zeng, L. M.: Influences of relative humidity and particle chemical composition on aerosol scattering properties during the 2006 PRD campaign, Atmos. Environ., 42, 1525–1536, 2008.

Lou, S., Holland, F., Rohrer, F., Lu, K., Bohn, B., Brauers, T., Chang, C. C., Fuchs, H., Häseler, R., Kita, K., Kondo, Y., Li, X., Shao, M., Zeng, L., Wahner, A., Zhang, Y., Wang, W., and Hofzumahaus, A.: Atmospheric OH reactivities in the Pearl River Delta – China in summer 2006: measurement and model results, Atmos. Chem. Phys., 10, 11243–11260, doi:10.5194/acp-10-11243-2010, 2010.

Lu, K. D., Zhang, Y. H., Su, H., Shao, M., Zeng, L. M., Zhong, L. J., Xiang, Y. R., Chang, C. C., Chou, C. K. C., and Wahner, A.: Regional ozone pollution and key controlling factors of photochemical ozone production in Pearl River Delta during summer time, Science China (Chemistry), 53, 651–663, 2010.

Mayer, S., Sandvik, A., Jonassen, O. M., and Reuder, J.: Atmospheric profiling with the UAS SUMO: a new perspectivefor the evaluation of fine-scale atmospheric models, Meteorol. Atmos. Phys., doi:10.1007/s00703-010-0063-2, 2010.

Miyazaki, Y., Kondo, Y., Shiraiwa, M., Takegawa, N., Miyakawa, T., Han, S., Kita, K., Hu, M., Deng, Z. Q., Zhao, Y., Sugimoto, N., Blake, D. R., and Weber, R. J.: Chemical characterization of water-soluble organic carbon aerosols at a rural site in the Pearl River Delta, China, in

ACPD
11, 4807–4842, 2011

the summer of 2006, J. Geophys. Res.-Atmos., 114, D14208, doi:10.1029/2009JD011736, 2009.

Miao, S. G., Chen, F., Margaret, A., LeMone, Tewari, M., Li, Q. C., and Wang, Y. C.: An Observational and Modeling Study of Characteristics of Urban Heat Island and Boundary Layer Structures in Beijing, J. Appl. Meteorol. Clim., 48, 484–501, 2009.

Nolan, S. D., Zhang, A. J., and Stern, P. D.: Evaluation of planetary boundary layer parameterizations in tropical cyclones by comparison of in situ observations and high-resolution simulations of hurricane Isabel (2003) – Part I: Initialization, maximum winds, and the outer-core boundary layer, Mon. Weather Rev., 137, 3651–3674, 2009a.

Nolan, S. D., Zhang, A. J., and Stern, P. D.: Evaluation of planetary boundary layer parameterizations in tropical cyclones by comparison of in situ observations and high-resolution simulations of hurricane Isabel (2003) – Part II: Inner-core boundary layer and eyewall structure, Mon. Weather Rev., 137, 3675–3698, 2009b.

Prtenjak, M. T., Jeričdević, A., Kraljević, L., Bulić, I. H., Nitis, T., and Klaić, Z. B.: Exploring atmospheric boundary layer characteristics in a severe SO_2 episode in the north-eastern Adriatic, Atmos. Chem. Phys., 9, 4467–4483, doi:10.5194/acp-9-4467-2009, 2009.

Rose, D., Nowak, A., Achtert, P., Wiedensohler, A., Hu, M., Shao, M., Zhang, Y., Andreae, M. O., and Pöschl, U.: Cloud condensation nuclei in polluted air and biomass burning smoke near the mega-city Guangzhou, China – Part 1: Size-resolved measurements and implications for the modelling of aerosol particle hygroscopicity and CCN activity, Atmos. Chem. Phys., 10, 3365–3383, doi:10.5194/acp-10-3365-2010, 2010.

Skamarock, W. C., Klemp, J. B., Dudhia, J., Gill, D. O., Barker, D. M., Wang, W., and Powers, J. G.: A description of the Advanced Research WRF Version 2, NCAR/TN-468+STR, Ncar Technical Note, 88 pp., available at: http://www.mmm.ucar.edu/wrf/users/docs/arw_v2.pdf, January 2007.

Verma, R. L., Sahu, L. K., Kondo, Y., Takegawa, N., Han, S., Jung, J. S., Kim, Y. J., Fan, S., Sugimoto, N., Shammaa, M. H., Zhang, Y. H., and Zhao, Y.: Temporal variation of elemental carbon in Guangzhou, China, in summer 2006, Atmos. Chem. Phys. Discuss., 9, 24629–24667, doi:10.5194/acpd-9-24629-2009, 2009.

Wu, D., Tie, X. X., Li, C. C., Ying, Z. M., Lau, A. K. H., Huang, J., Deng, X. J., and Bi, X. Y.: An extremely low visibility event over the Guangzhou region: a case study, Atmos. Environ., 39, 6568–6577, 2005.

Xiao, R., Takegawa, N., Kondo, Y., Miyazaki, Y., Miyakawa, T., Hu, M., Shao, M., Zeng, L. M.,

ACPD
11, 4807–4842, 2011

Hofzumahaus, A., Holland, F., Lu, K., Sugimoto, N., Zhao, Y., and Zhang, Y. H.: Formation of submicron sulfate and organic aerosols in the outflow from the urban region of the Pearl River Delta in China, Atmos. Environ., 43, 3754–3763, 2009.

Yu, H., Wu, C., Wu, D., and Yu, J. Z.: Size distributions of elemental carbon and its contribution to light extinction in urban and rural locations in the pearl river delta region, China, Atmos. Chem. Phys., 10, 5107–5119, doi:10.5194/acp-10-5107-2010, 2010.

Yu, S., Eder, B., Dennis, R., Chu, S. H., and Schwariz, S.: On the development of new metrics for the evaluation of air quality models, Atmos. Sci. Lett., 7, 26–34, 2005.

Zhang, Y. H., Su, H., Zhong, L. J., Cheng, Y. F., Zeng, L. M., Wang, X. S., Xiang, Y. R., Wang, J. L., Gao, D. F., Shao, M., Fan, S. J., and Liu, S. C.: Regional ozone pollution and observation-based approach for analyzing ozone–precursor relationship during the PRIDE-PRD2004 campaign, Atmos. Environ., 42, 6203–6218, 2008a.

Zhang, Y. H., Hu, M., Zhong, L. J., Wiedensohlerg, A., Liu, S. C., Andreae, M. O., Wang, W., and Fan S. J.: Regional integrated experiments on air quality over Pearl River Delta 2004 (PRIDE-PRD2004): overview, Atmos. Environ., 42, 6157–6173, 2008b.

Zhu, P.: A multiple scale modelling system for coastal hurricane wind damage mitigation, Nat. Hazards, 47, 577–591, 2008.

ACPD
11, 4807–4842, 2011

Table 1. The statistic parametres between the measured 2-m air temperature (T), wind speed (WS) and wind direction (WD), respectively, and the modelled by WRF model during 12–15 July 2006 (period I), 15–18 July 2006 (period II) and 20–23 July 2006 (period III).

	I			II			III		
	WD	WS	T	WD	WS	T	WD	WS	T
Mean observable	254.0	2.97	30.86	169.3	3.06	27.29	176.6	1.83	30.09
Mean simulation	257.9	3.88	29.78	187.6	7.45	27.99	172.0	2.18	28.73
R	0.46	0.42	0.72	0.45	0.39	0.49	0.61	0.43	0.93
MB	3.92	0.91	−1.08	18.33	4.39	0.70	−4.57	0.35	−1.26
MAGE	36.34	1.78	1.80	39.02	4.47	1.29	52.88	0.99	1.31
RMSE	51.07	2.19	2.19	47.39	4.96	1.53	69.92	1.22	1.63
FAE (%)	4.1	14.0	1.5	6.0	21.9	1.2	8.7	14.7	1.2

ACPD
11, 4807–4842, 2011

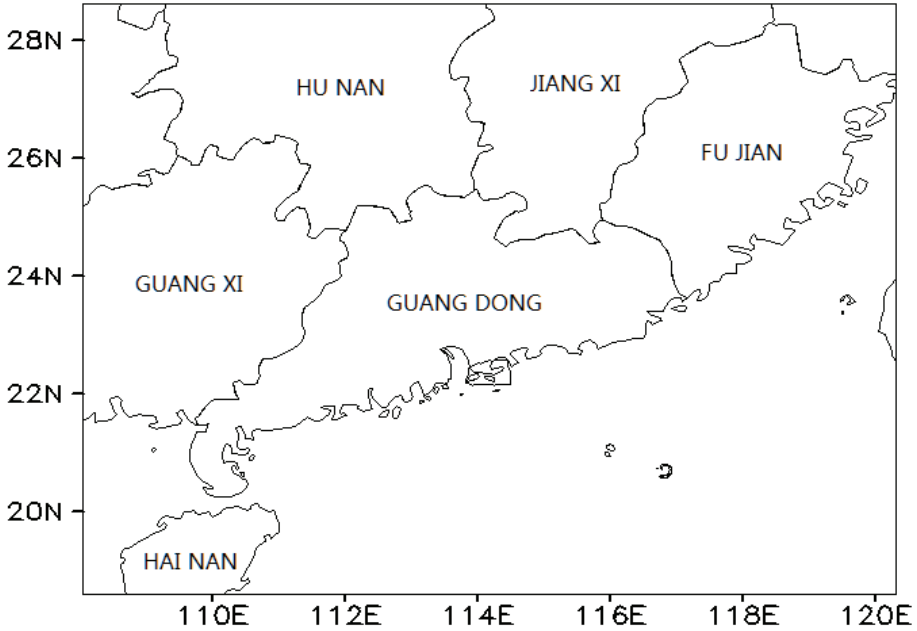

Fig. 1a. Map of the Guangdong province and its surroundings.

ACPD
11, 4807–4842, 2011

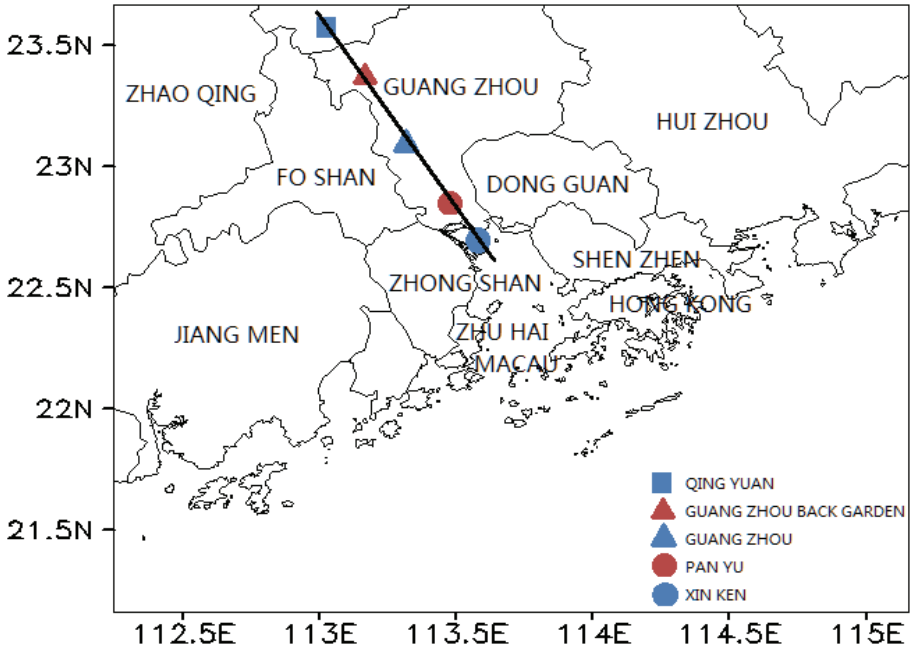

Fig. 1b. Map of PRD area. The sites of measurements are showed.

ACPD
11, 4807–4842, 2011

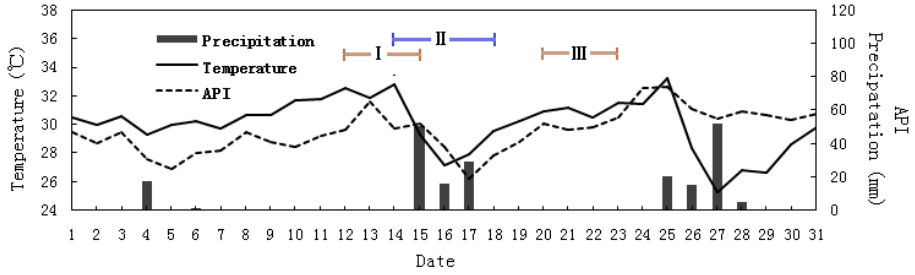

Fig. 2. The measured temperature, precipitation and air pollution index (API) at Guangzhou station during July 2006 (I: 12 July to 15 July; II: 14 July to 18 July; III: 20 July to 23 July).

ACPD
11, 4807–4842, 2011

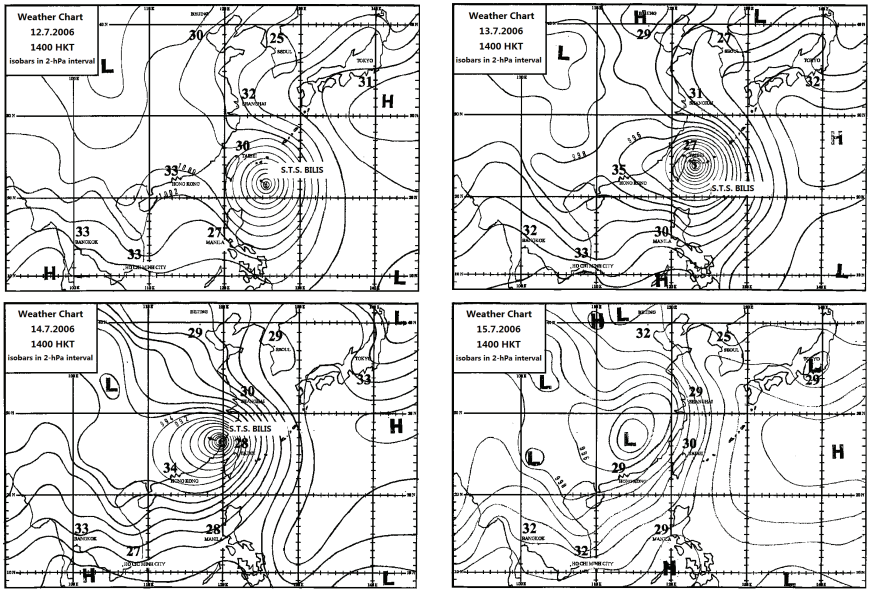

Fig. 3. The surface weather situation during 12–15 July 2006.

ACPD
11, 4807–4842, 2011

Atmospheric boundary layer characteristics over PRD

S. J. Fan et al.

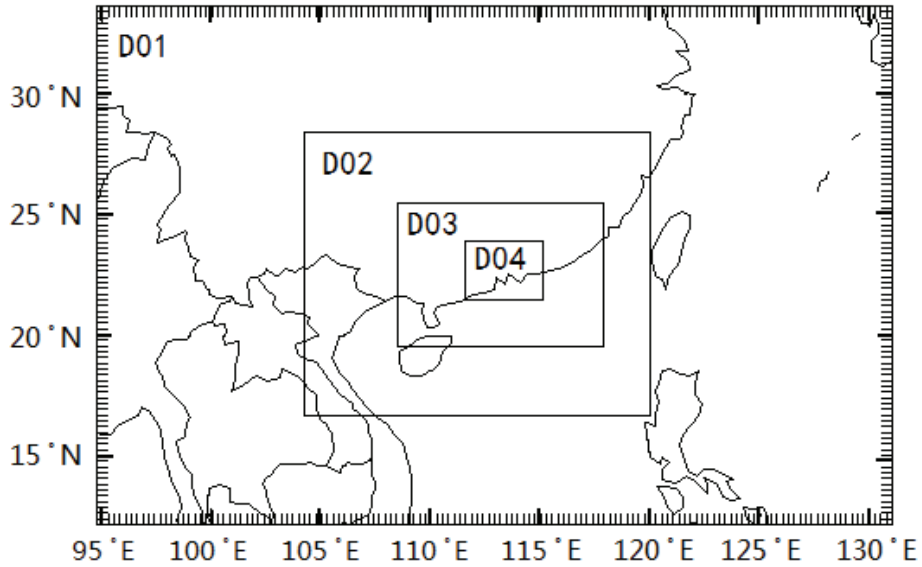

Fig. 4. Domain settings in WRF model.

ACPD
11, 4807–4842, 2011

Fig. 5. The observed and simulated 2-m temperature, wind speed and wind direction at Guangzhou from 12 July to 15 July.

ACPD
11, 4807–4842, 2011

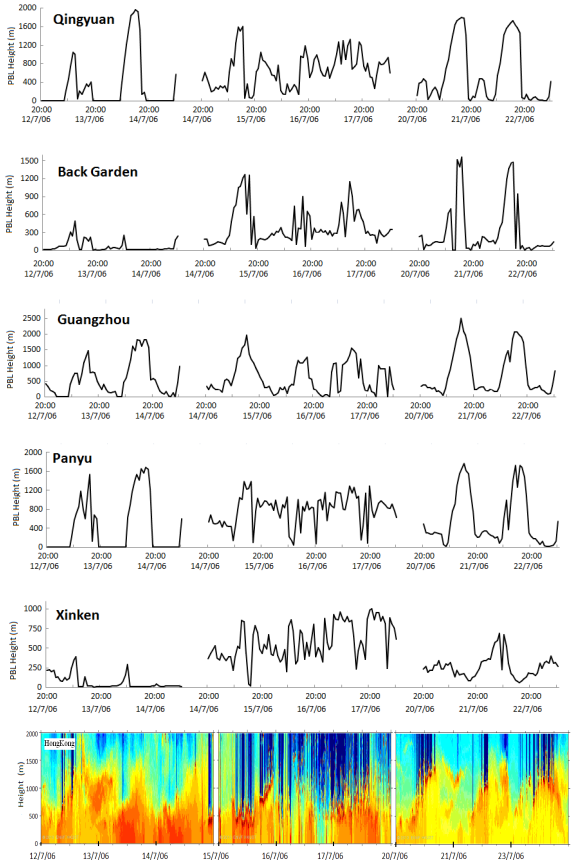

Fig. 6. The variation of the modelled WRF atmospheric boundary layer height (m) for Qingyuan, Back garden, Guangzhou, Panyu and Xinken stations, and the Lidar normalized relative backscattering signal at YuenLong station in Hongkong.

ACPD
11, 4807–4842, 2011

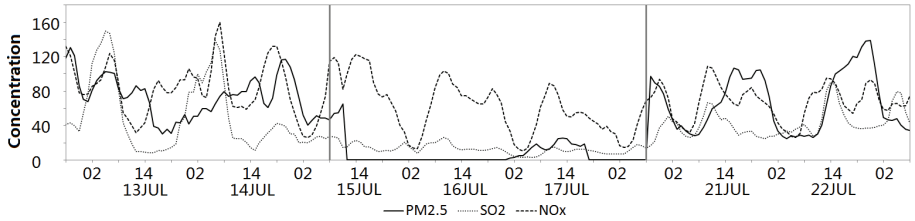

Fig. 7. The measured air pollutant concentrations at Guangzhou station from 13 July to 22 July (unit: $PM_{2.5}$: mg/m^3, SO_2: ppb, NO_x: ppb).

ACPD
11, 4807–4842, 2011

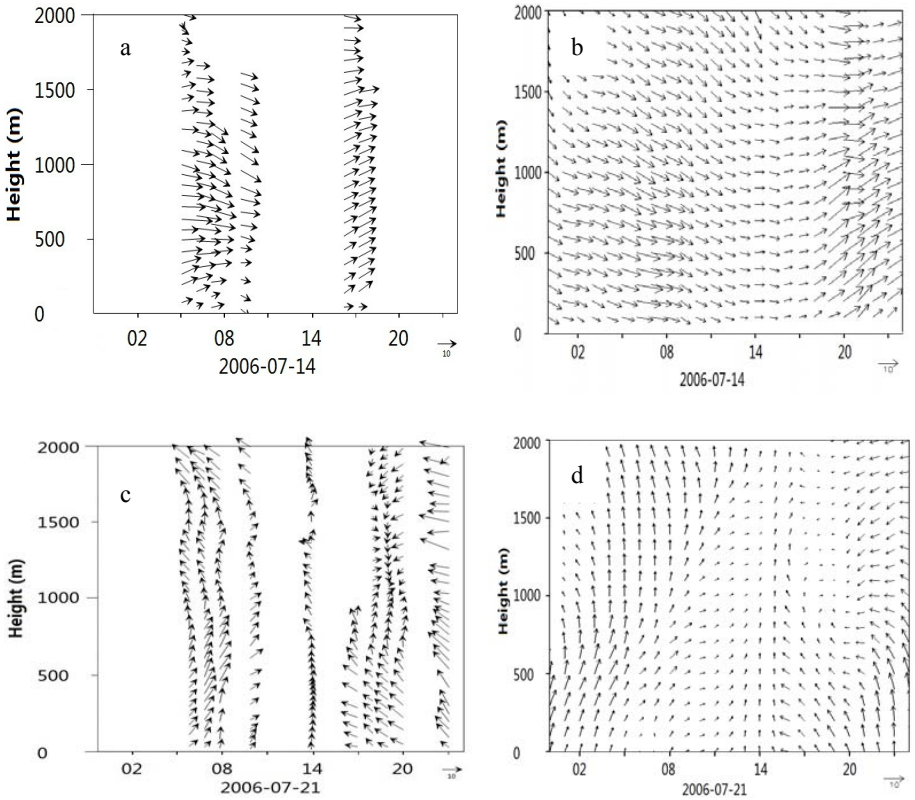

Fig. 8. The vertical wind profile by radio sounding at Panyu station on 14 July and 21 July (**(a)**: observations on 14 July, **(b)**: simulations on 14 July, **(c)**: observations on 21 July, **(d)**: simulations on 21 July).

ACPD
11, 4807–4842, 2011

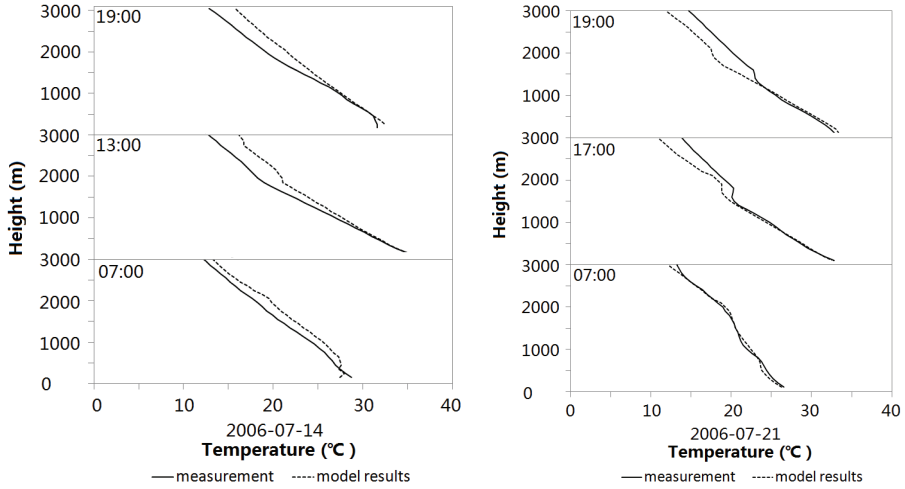

Fig. 9. The measured vertical temperature profile by radar sounding and the modelled results at Qingyuan station on 14 July and 21 July.

ACPD
11, 4807–4842, 2011

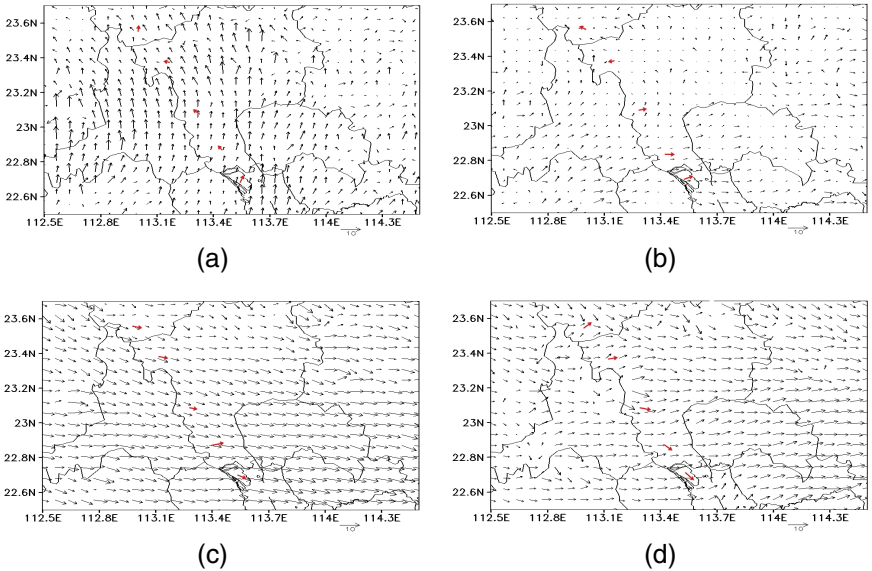

Fig. 10. The measured (red arrows) 10-m wind (ms-1) from main meteorological stations in Fig. 1b and modelled WRF wind field (black arrows) in PRD region (**(a)**: 20:00 LST on 12 July, **(b)**: 02:00 LST on 13 July, **(c)**: 08:00 LST on 14 July, **(d)**: 14:00 LST on 14 July).

ACPD
11, 4807–4842, 2011

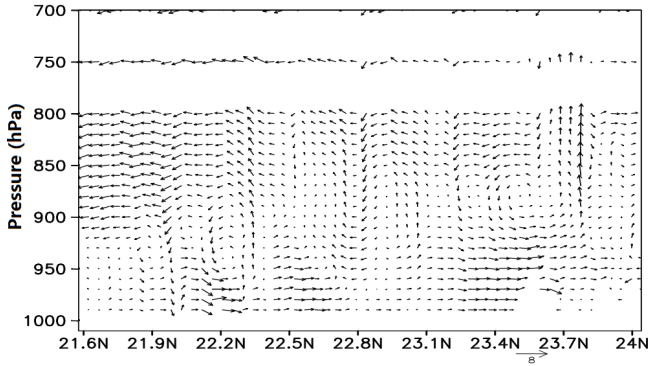

(a)

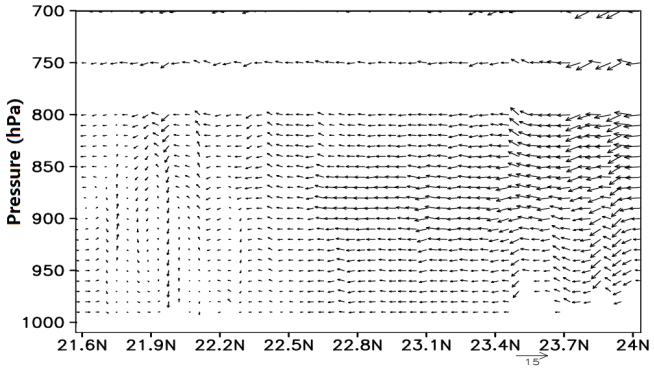

(b)

Fig. 11. Vertical cross-sections of the WRF modelled wind ($m\,s^{-1}$) along 113.2° E at 03:00 LST on 13 July **(a)** and 03:00 LST on 14 July **(b)**.

ACPD
11, 4807–4842, 2011